NANO · MICRO
small

Supporting Information

for *Small*, DOI 10.1002/smll.202308293

Construction of Hierarchical Films via Layer-by-Layer Assembly of Exfoliated Unilamellar Zeolite Nanosheets

*Chenhui Wang, Nobuyuki Sakai, Yasuo Ebina, Takayuki Kikuchi, Justyna Grzybek, Wieslaw J. Roth, Barbara Gil, Renzhi Ma and Takayoshi Sasaki**

Supporting Information

Construction of Hierarchical Films via Layer-by-Layer Assembly of Exfoliated Unilamellar Zeolite Nanosheets

*Chenhui Wang, Nobuyuki Sakai, Yasuo Ebina, Takayuki Kikuchi, Justyna Grzybek, Wieslaw J. Roth, Barbara Gil, Renzhi Ma, and Takayoshi Sasaki**

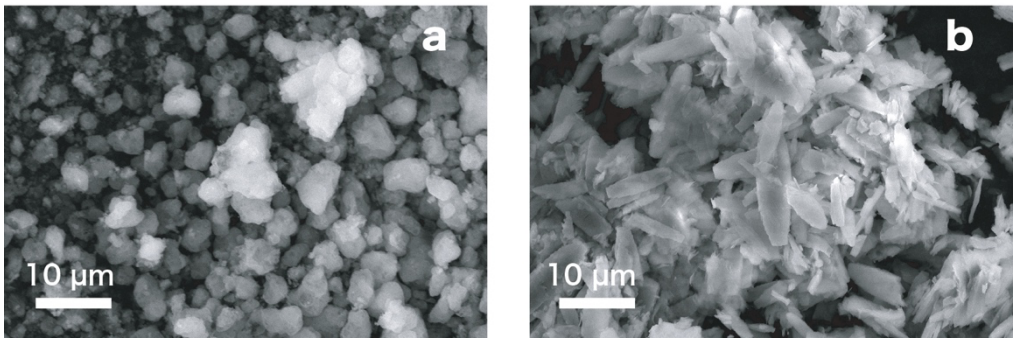

Figure S1. SEM images of a) MCM-56 and b) Al-ZSM-55.

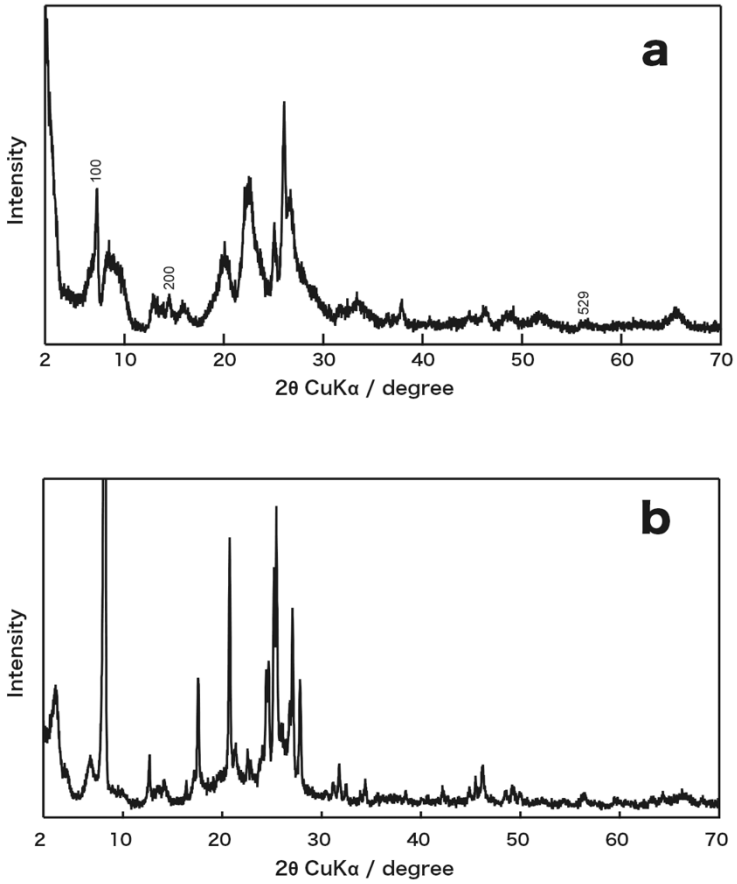

Figure S2. XRD patterns of a) MCM-56 and b) Al-ZSM-55. The former data can be ascribed to the disordered hexagonal structure without layer-to-layer registry. The latter is a mixture of the layered precursor to zeolite CDO designated ZSM-55 (unexfoliable) and bifer (exfoliable).

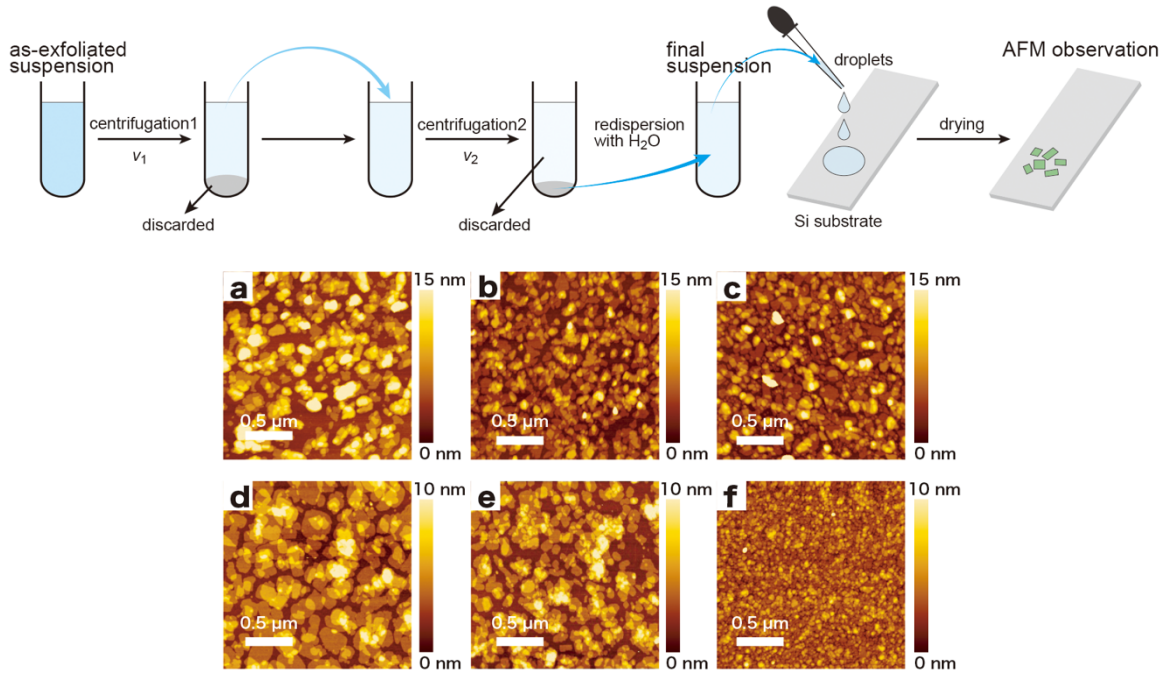

Figure S3. Schematic illustration of collecting the unilamellar nanosheets from the as-prepared suspension and AFM images of a–c) mww and d–f) bifer samples from the final suspension. The samples (a,d) are obtained with v_1 = 10 krpm and v_2 = 20 krpm, and (b,e) are with v_1 = 20 krpm and v_2 = 30 krpm. The images (c,f) are from the top suspensions obtained with v_1 = 20 krpm and v_2 = 30 krpm.

The as-exfoliated suspensions contain various species such as few-layer nanosheets and small cracked fragments besides monolayer nanosheets as the fully exfoliated product. The suspensions are subject to two-step centrifugation at different rotation speeds (see the scheme in Figure S3) to separate them. Drops of a resulting suspension are dried on an Si wafer and the nanosheet quality is characterized by atomic force microscopy (AFM) observation. As shown in Figure S3a, the suspension obtained with v_1 = 10 krpm and v_2 = 20 krpm contains a large amount of sheet-like particles thicker than a dozen of nanometers, indicating that the multilayer MWW zeolite (unexfoliated portion) is not removed by this process. The sample obtained with v_1 = 20 krpm and v_2 = 30 krpm exhibits a uniform and monolayer thickness of mww nanosheets as a major product (Figure S3b), while the sample obtained by drying the top suspensions with v_1 = 20 krpm and v_2 = 30 krpm shows fine dots, suggesting the presence of small unexfoliated MWW zeolite (Figure S3c). For bifer nanosheets, the sample obtained with v_1 = 10 krpm and v_2 = 20 krpm exhibits a high quality of uniform and monolayer thickness with relatively large lateral size (Figure S3d), while the other two samples show a smaller nanosheet (Figure S3e) and even a small dot (Figure S3f), respectively.

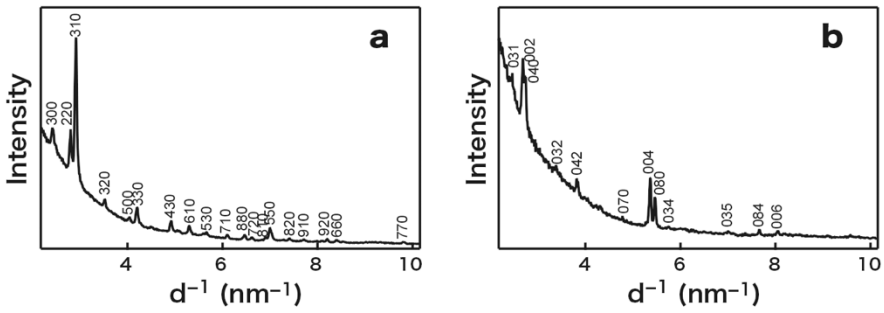

Figure S4. In-plane XRD data of a) mww and b) bifer nanosheets.

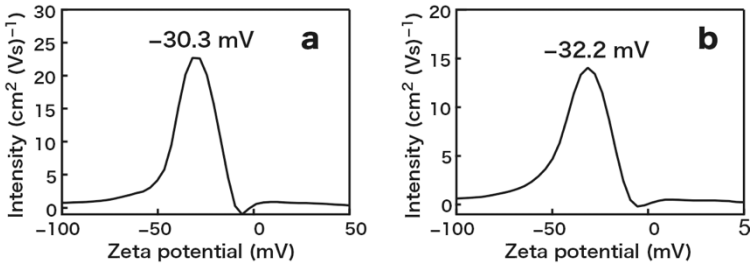

Figure S5. Zeta potentials of a) mww and b) bifer nanosheet suspensions.

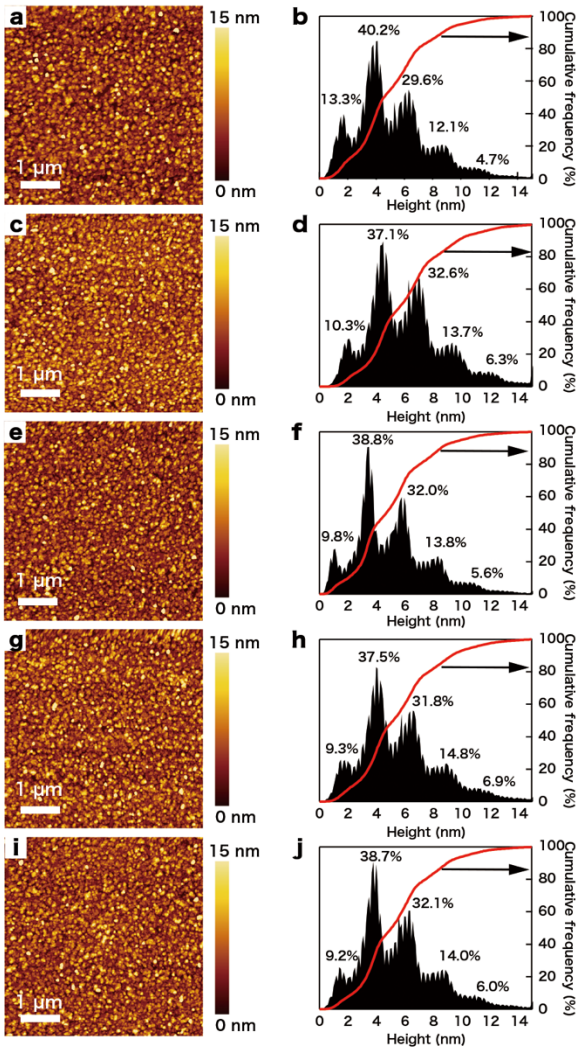

Figure S6. AFM images and corresponding height histograms of the mww films fabricated with the concentration of 0.08 g dm^{-3} and the deposition time of a,b) 5 min, c,d) 10 min, e,f) 15 min, g,h) 20 min, and i,j) 30 min.

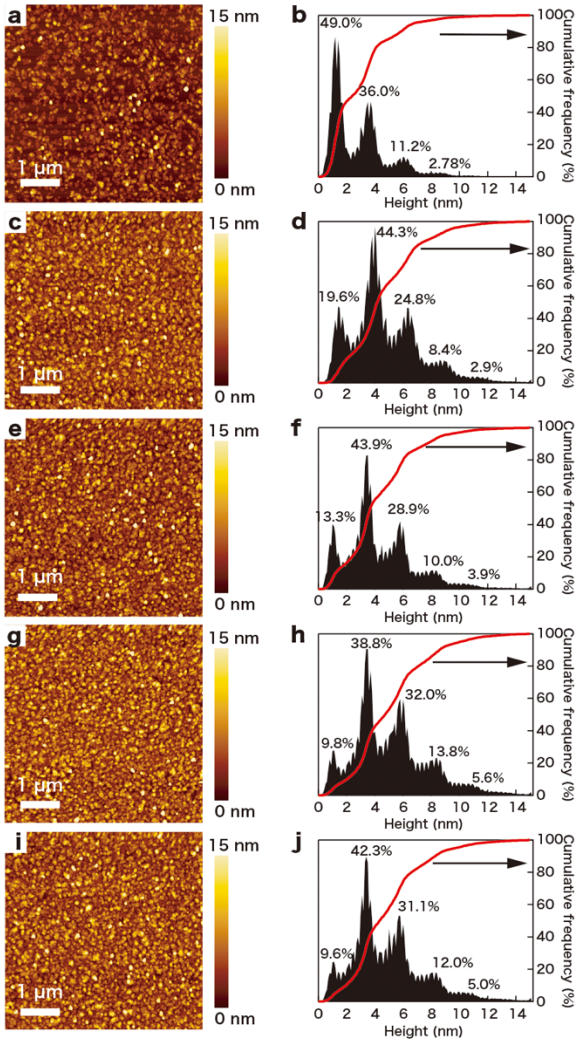

Figure S7. AFM images and corresponding height histograms of the mww films fabricated with the deposition time of 15 min and the concentration of a,b) 0.02 g dm^{-3}, c,d) 0.04 g dm^{-3}, e,f) 0.06 g dm^{-3}, g,h) 0.08 g dm^{-3}, and i,j) 0.10 g dm^{-3}.

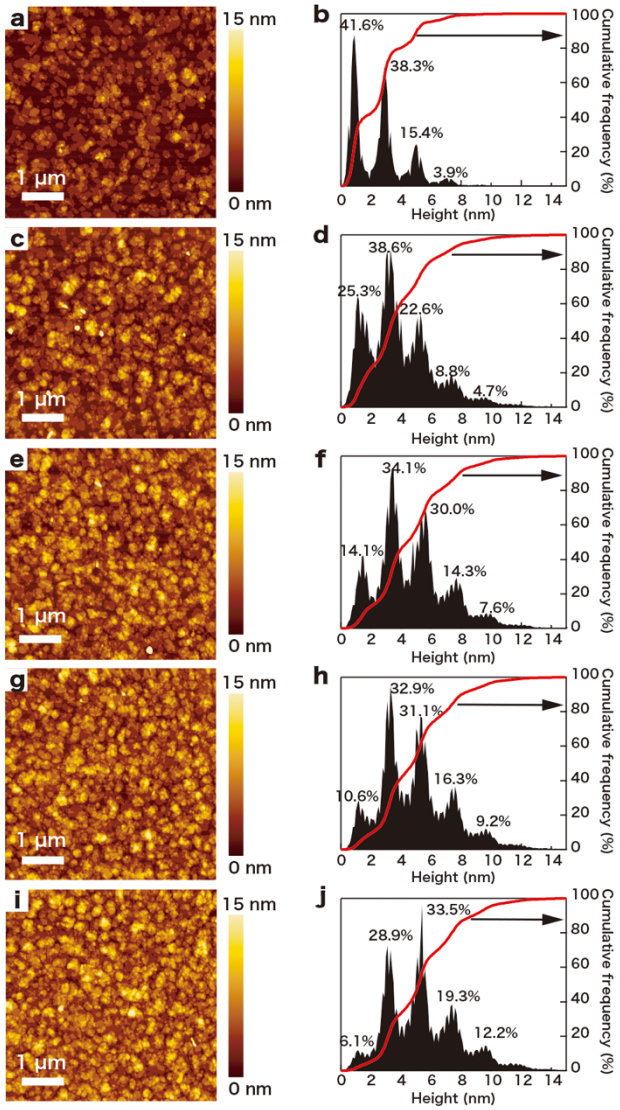

Figure S8. AFM images and corresponding height histograms of the bifer films fabricated with the concentration of 0.08 g dm^{-3} and the deposition time of a,b) 5 min, c,d) 10 min, e,f) 15 min, g,h) 20 min, and i,j) 30 min.

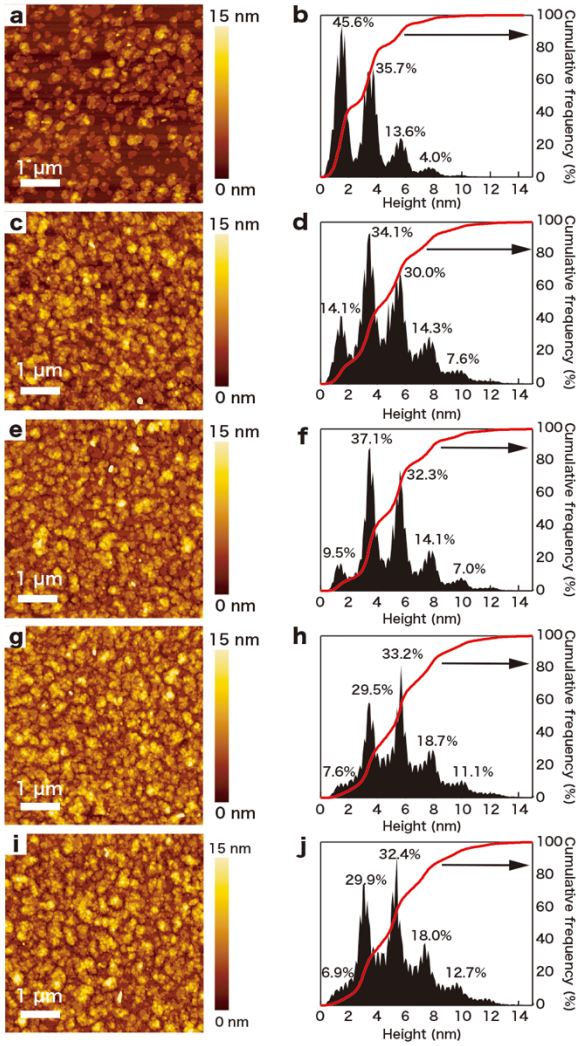

Figure S9. AFM images and corresponding height histograms of the bifer films fabricated with the deposition time of 15 min and the concentration of a,b) 0.04 g dm^{-3}, c,d) 0.08 g dm^{-3}, e,f) 0.12 g dm^{-3}, g,h) 0.20 g dm^{-3}, and i,j) 0.28 g dm^{-3}.

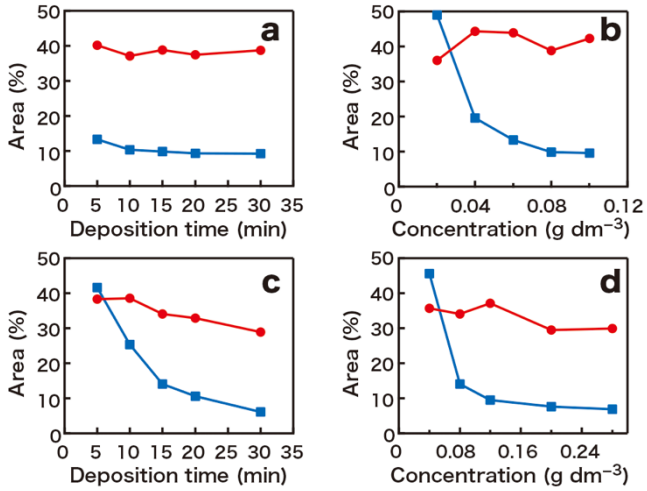

Figure S10. The ratios of uncovered area (blue) and monolayer region (red) of a,b) mww and c,d) bifer films fabricated with a,c) the concentration of 0.08 g dm^{-3} and b,d) the deposition time of 15 min.

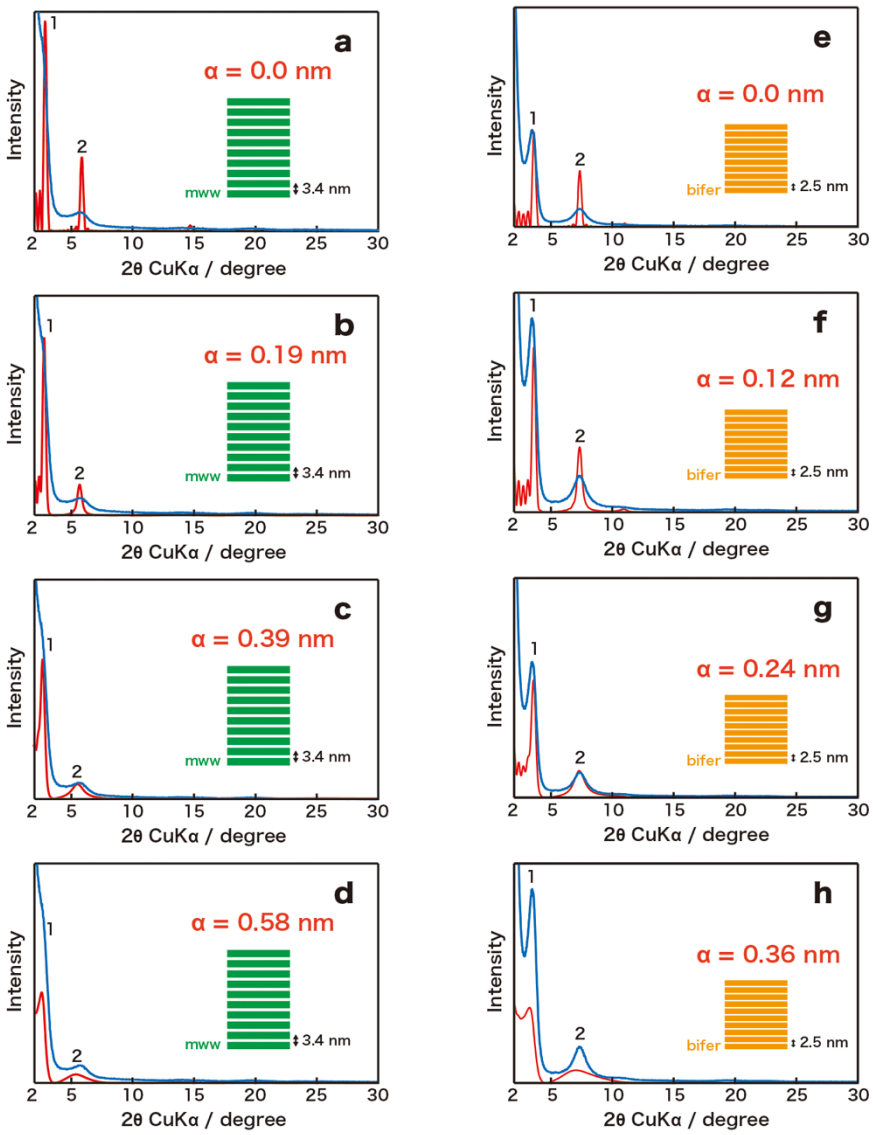

Figure S11. Measured (blue line) and simulated XRD (red line) patterns of a–d) mww and e–h) bifer nanosheets. The digits indicate the order of reflection. The lattice distortion parameter, α, is varied to obtain a good fit to the experimental profile.

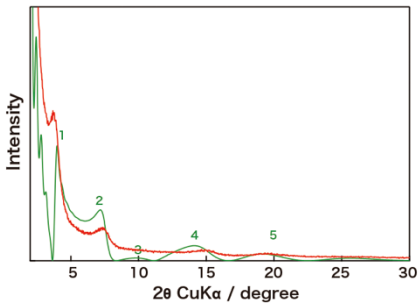

Figure S12. XRD (red line) and simulated XRD (green line) patterns of heated multilayer films of mww. Simulation parameters are $N = 10$ and $\alpha = 0.22$ nm.

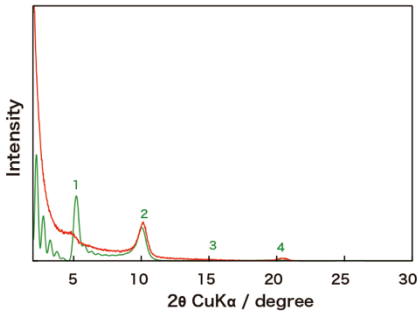

Figure S13. XRD (red line) and simulated XRD (green line) patterns of heated multilayer films of bifer. Simulation parameters are $N = 10$ and $\alpha = 0.11$ nm.

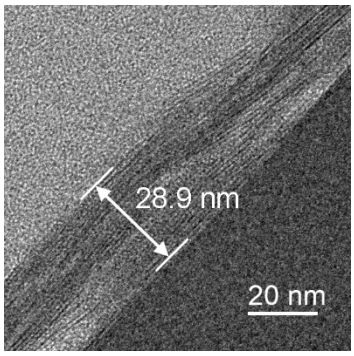

Figure S14. TEM image of a film of (mww/bifer)$_5$ on ITO substrate.

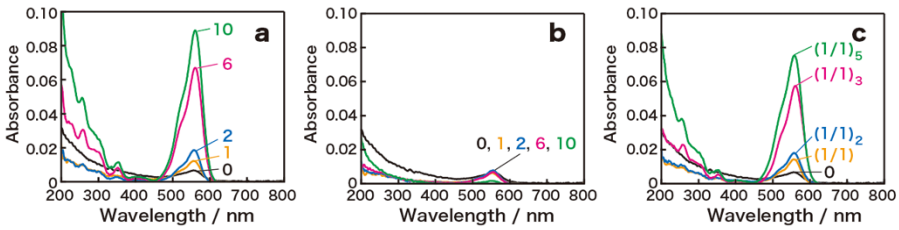

Figure S15. UV-vis absorption spectra of the zeolite films after treating with the Rhodamine B dye, a) mww film, b) bifer film, and c) mww/bifer with different layers.

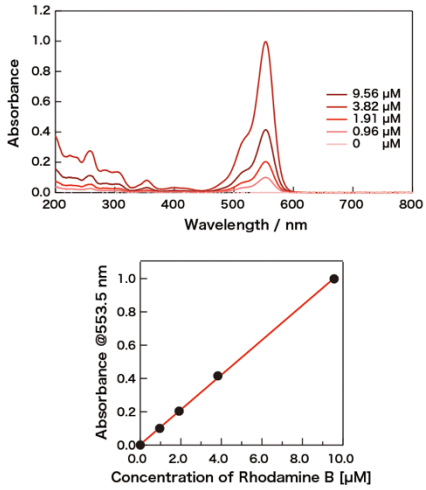

Figure S16. UV-vis absorption spectra of aqueous solutions of Rhodamine B at various concentrations.

The absorbance shows linear relationship as a function of the concentration, following the Beer's law, and the molar extinction at 553.5 nm is calculated as 1.05×10^5 mol^{-1} dm^3 cm^{-1}. A slight shift in peak-top wavelength may be associated with some difference of the dye molecules in aqueous solution and the film. By assuming that such a minor difference can be neglected, the amount of dye in the film can be estimated on the basis of the obtained molar extinction coefficient.

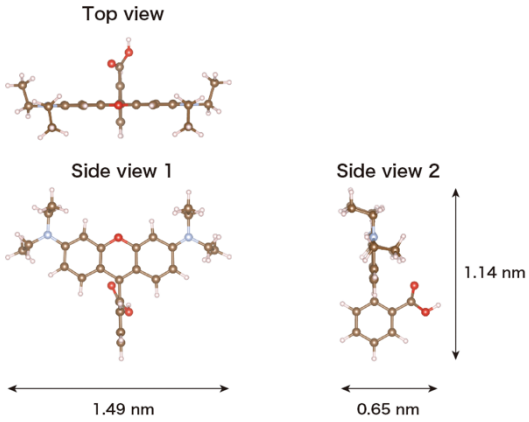

Figure S17. Molecular structure of Rhodamine B.

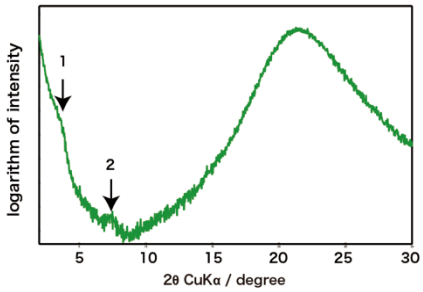

Figure S18. XRD data of the 10-layer film of mww on a quartz glass substrate after the adsorption of Rhodamine B.

The peaks indicated by numerals 1 and 2 are the basal reflections, corresponding to the interlayer distance of 2.3 nm. This value is the same as that for the 10-layer film of mww nanosheets heated at 400 °C for 24 h (Figure 5a), indicating a negligible change in the structure upon the treatment with the dye solution. The peaks are rather broad and weak, which may be due to the fact that the film samples for the dye adsorption are fabricated on a quartz glass substrate. The broad hump at 15–30 degree in 2θ is attributable to amorphous halo from the quartz glass.